*Journal of the Meteorological Society of Japan*, Vol. 74, No. 4, pp. 399–413, 1996 

# Role of the Northeast Winter Monsoon on the Biennial Oscillation of the ENSO/Monsoon System

**By Tomohiko Tomita**

*Department of Atmospheric Sciences, University of California at Los Angeles, Los Angeles, CA 90095–1565, USA*

**and**

**Tetsuzo Yasunari**

*Institute of Geoscience, University of Tsukuba, Tsukuba, Ibaraki 305, Japan*

*(Manuscript received 11 May 1995, in revised form 20 May 1996)*

## Abstract

The diagnostic study of the biennial oscillation (BO) of the ENSO/monsoon system is performed by using the sea surface temperature (SST), sea surface wind, sea level pressure, and outgoing longwave radiation data.

The BO is a prominent feature of the ENSO/monsoon system that results in the modulation of convective activity aroud the maritime continent. The BO tends to change its anomalous states during the Northern Hemisphere spring. The SST variation around the South China Sea also has a BO with a phase transition that tends to occur about a half year earlier, that is, during the Northern Hemisphere autumn. The intensification of the northeast winter monsoon (NEWM) probably modifies the anomalous state of the SST which persists until the northern summer.

The SST anomalies around the South China Sea are favorable for modifying the convective activity around the maritime continent during the northern winter to summer. The strength of the convective activity further regulates the SST anomalies in the tropical central-eastern Pacific through the Walker circulation during the northern summer to winter. This anomalous SST state is probably responsible for the strength of the NEWM by controlling the extratropical circulation pattern. The NEWM changes the anomalous state of the SST around the South China Sea. Thus the cycle of the BO of the ENSO/monsoon system is completed. It is, thus, strongly suggested that the tropical-extratropical interaction plays an essential role in the BO of the ENSO/monsoon system.

## 1. Introduction

The maritime continent, *i.e.*, the tropical region with many islands in and around the area of Southeast Asia, is the world's most dominant center of convective activity which is maintained by the world's highest sea surface temperature (SST) of over 28.0°C. A number of recent studies (Barnett, 1983; Rasmusson and Carpenter, 1983; Mooley and Shukla, 1987; Yasunari, 1990; Joseph *et al.* , 1991; Webster and Yang, 1992; Joseph *et al.*, 1994, among others) have demonstrated the close link between the El Niño/Southern Oscillation (ENSO) phenomenon and the Asian monsoon which is attributed to convective activity. In the present study, the term "ENSO/monsoon system" is used as a large-scale air-sea-land interaction system related through this convective activity.

The biennial oscillation (BO) and/or the quasi-biennial oscillation (QBO) of the convective activity have been recognized as important fluctuations of the ENSO/monsoon system (Yasunari, 1987; Barnett, 1991). Rasmusson *et al.* (1990), by use of a spectral analysis, revealed the existence of the BO (or QBO) in the SST and wind variations near the maritime continent, which is strongly phase-locked with the annual cycle. Meehl (1987, 1993) specifically demonstrated that the BO occurred as an interactive process between the seasonal march of convective activity around the maritime continent and the accumulation of heat in the surface

mixed layer of the tropical western Pacific and the tropical eastern Indian Oceans. From the results of a general circulation model, Meehl (1994) further pointed out the importance of soil moisture anomaly in South Asia, and suggested that the tropical-extratropical interaction was responsible for the circulation anomalies over Asia that maintained the land surface temperature anomalies during winter and spring. He suggested that the tropical-extratropical interaction might be an essential part of the BO in terms of the circulation pattern over Asia.

Based on the global-scale statistical analyses of SST, sea level pressure (SLP), and the surface zonal wind, Barnett (1991) and Ropelewski *et al.* (1992) revealed the global BO pattern and the interannual LF (low-frequency) fluctuation. The former pattern was quasi-progressive from the Indian Ocean to the Pacific Ocean while the latter pattern had a 4–5-year period resembling a standing seesaw between the maritime continent or the western tropical Pacific and the tropical eastern Pacific. Yasunari and Seki (1992) investigated the mechanism of the BO process by considering the link between the tropics and mid-high latitudes, with specific emphasis on the snow cover over central Asia. Yasunari (1991) proposed a concept of "the monsoon year," defined by the strength of the Asian summer monsoon, which was appropriate for describing the seasonal march of the annual anomalous states of tropical climate. Shen and Lau (1995) further revealed the BO relationship between precipitation in the eastern and eastern south China and the SST of the equatorial Pacific and Indian Oceans.

Based on a simple BO model, Nicholls (1978) showed that the tropospheric BO around the Indonesia-northern Australia region resulted from interactions of the seasonal change of the wind with relevant variations of the SST and SLP. Brier (1978) also proposed a conceptual BO model which had seasonal air-sea interactions. In these models, it was crucial for the appearance of the BO that a negative interaction or feedback occurred in the seasonal air-sea interactions, while positive interactions occurred during the other seasons. Lau and Sheu (1988) further extended this conceptual model to the ENSO cycle having a 4-year period.

The BO has been explored in terms of many climatic elements since the 1960s to clarify the relationship between the tropospheric BO and the tropical lower stratospheric QBO in the zonal wind (Angell *et al.*, 1966; Ananthakrishnan and Thiruvengadathan, 1966; Angell and Korshover, 1968, Angell *et al.*, 1969; Newell *et al.*, 1969; Ebdon, 1975; Angell and Korshover, 1977; Yasunari, 1989 among others). Several other studies (*cf.* Trenberth, 1980; Barnett, 1991; Xu, 1992), however, have denied or questioned the existence of the troposphere-stratosphere link.

The purpose of this study is to describe the tropospheric BO processes of the ENSO/monsoon system in more detail, emphasized on the phase change processes. Meehl (1993) questioned why the phase change occurred only during the boreal spring, although convective activity around the maritime continent passes over the equator twice yearly. This question strongly suggests that there might be an additional process that had not been included in Meehl's BO model. This study will propose a new process for the phase change of the BO through further elaboration on the tropical-extratropical interaction over the Pacific, and will inspect the suggestion of Meehl (1994).

The data presently used are described in Section 2, while Section 3 shows the relationship between the BOs of the SST in the South China Sea and the Indian southwest monsoon. Section 4 describes the temporal and spatial BO developments based on the SST, wind, SLP, and outgoing longwave radiation (OLR). Conclusions are given in Section 5.

The present study makes use of the northeast winter monsoon (NEWM) and the Indian southwest monsoon (ISWM), which have been defined in Fein and Stephens (1987), specifically. The seasons referred to in the text are for the Northern Hemisphere, unless otherwise noted.

## 2. Data

The following five datasets were used in the analyses of the present study:

(1) All-India monthly rainfall data listed in Parthasarathy *et al.* (1994). This dataset covers the 123-year period from 1871 to 1993. The data are based on the area-weighted average of 306 well-distributed raingauge stations over the entire Indian subcontinent. For details, see Mooley and Parthasarathy (1984) and Parthasarathy *et al.* (1991, 1994). The dataset provides a good measure of the strength of the Indian summer monsoon (ISM) over a long period of more than 100 years.

(2) The SST data edited by the United Kingdom Meteorological Office. The spatial resolution of this dataset is 5° latitude by 5° longitude, covering most of the globe (all longitudes, 80°N–80°S). The time resolution is monthly and the period covered is from 1854 through 1993. The data for 1950–1990 are used for analyses due to the number of missing data prior to 1950.

(3) The wind data edited from the Comprehensive Ocean-Atmosphere Data Set. The data were rearranged to monthly during the period 1950–1990 and to a 5°×5° lat.-lon. grid south of 70°N over the global oceans. For details, refer to Iwasaki and Hanawa (1990) and Hanawa *et al.* (1995).

(4) The sea level pressure (SLP) data for the Northern Hemisphere. The dataset was edited by the National Center for Atmospheric Research. The

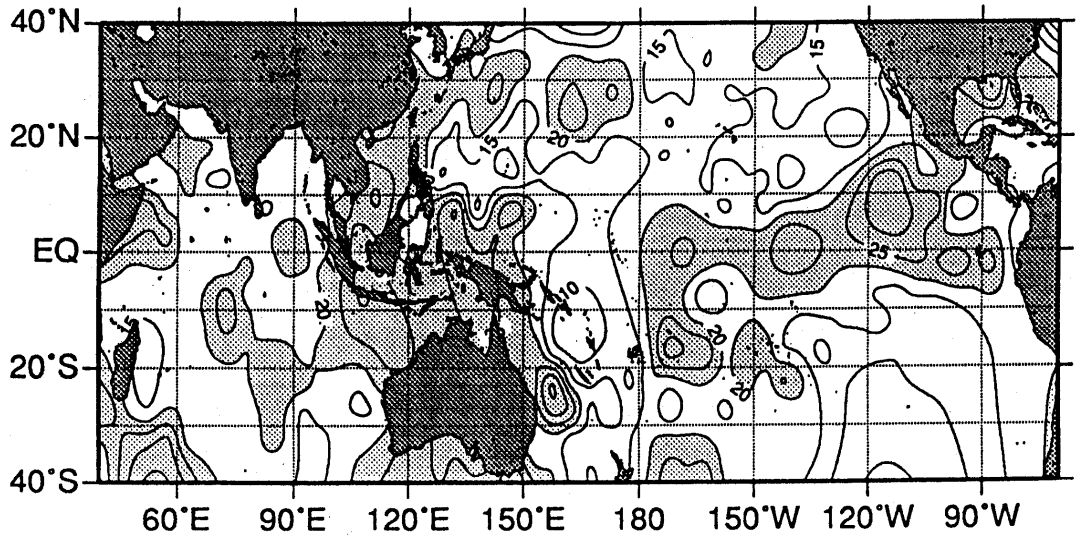


Fig. 1. Percentage of the SST variance of band-pass filtered BO anomalies (18–36 month period) to the interannual variability, in units of percent. The contour interval is 5 %. Areas greater than 20 % are shaded. The band-pass filter used is that of Murakami (1979).

grid intervals are 5°×5°, with monthly data covering the 48 years from 1946 to 1993.

(5) Global daily mean outgoing longwave radiation (OLR) data. The National Meteorological Center/National Oceanic and Atmospheric Research edited the original dataset. The data used in the present study were reduced to daily data from the original twice-daily data at the spatial resolution of 2.5° lat.-long. grid for the 14-year period of 1975–1989 (except for 1978).

## 3. Biennial oscillations of the SST around the South China Sea and the Indian southwest monsoon

The results of spectral analyses have revealed that a number of climatic elements or indicators relevant to the ENSO/monsoon system exhibit remarkable biennial oscillation (BO) components, *i.e.*, the Southern Oscillation index (SOI), SST in the central equatorial Pacific, and rainfall in the tropical central-western Pacific (Rasmusson and Carpenter, 1982; Lau and Sheu, 1988; Rasmusson *et al.*, 1990; Ropelewski *et al.*, 1992; Shen and Lau, 1995).

With respect to the SST variation, Fig. 1 shows the percentage of the variance of band-pass filtered BO anomalies (18–36-month period) to the total variance of interannual variability. Ropelewski *et al.* (1992) and Shen and Lau (1995) showed the similar figures, except that the percentages were for the SST variance associated with the annual cycle to the total SST variance. In Fig. 1, two areas of large percentage can be seen, *i.e.*, in the tropical central-eastern Pacific, and around the maritime continent which includes the regions from the East China Sea to the Arafura Sea. The former is closely related to the ENSO event (Barnett, 1991; Ropelewski *et al.*, 1992; Tomita and Yasunari, 1993), while the latter is probably related to the BO of the Asian/Australian monsoon judging from its geographical extent.

The curves (a) and (b) in Fig. 2 display the interannual variabilities of SST in the South China Sea and the All-India rainfall, respectively. The South China Sea is adopted as representative of the relatively large area around the maritime continent shown in Fig. 1. The two time series indicated by the solid lines appear to have a dominant interannual variability with a 2–3-year period and a phase lag of approximately a half year. Moreover, the maximum and minimum peaks tend to appear during the northern winter (a) and in the northern summer in (b). The band-pass filtered anomalies (18–36-month period) represented by the dashed lines strongly support these features.

In order to reveal the dominant periodicity more accurately, a power spectral analysis was applied to the two time series indicated by the solid lines in Fig. 2. The SST in the South China Sea exhibits significant power spectral density at periods of 25–29-months in its interannual variability (Fig. 3a). The interannual variability of the All-India rainfall also displays significant power over the period range of less than 3 years (Fig. 3b).

With respect to the power shown in Fig. 3a, the interannual variability of meridional wind component over the South China Sea (100°E–130°E, EQ–30°N) manifests the dominant periods around 24-months and 40-months (Fig. 3c). Figure 3d also exhibits significant power at periods of 22-months and 40-months in the interannual variability of the pressure difference between 80°E–110°E, 40°N–60°N,

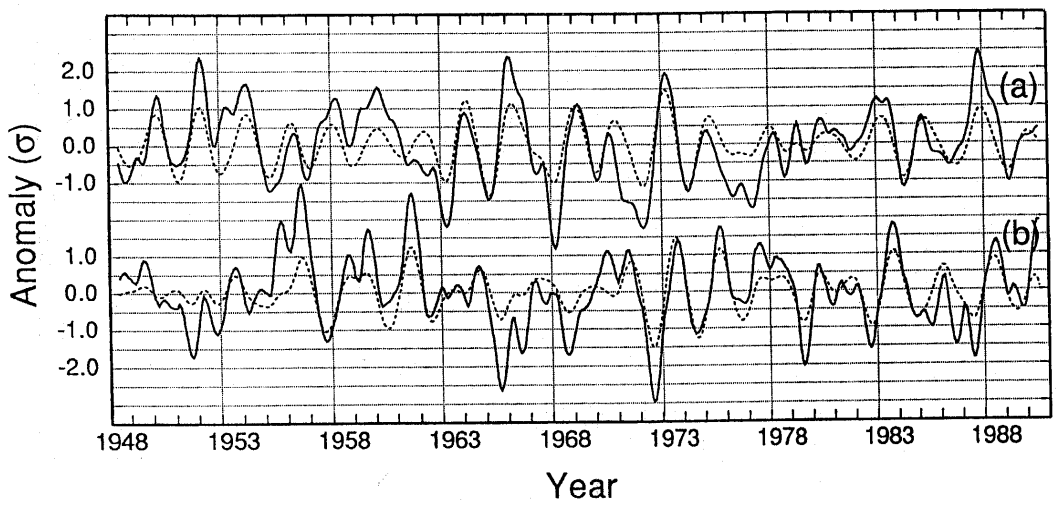


Fig. 2. Normalized interannual variabilities of SST in the South China Sea (100–120°E, EQ-25°N) and All-India rainfall indicated by the solid lines in curves (a) and (b), respectively, and band-pass filtered BO anomalies (18–36 month period) (dashed lines). The long-term trend and annual cycles have been removed by subtracting the linear trend and the monthly mean values. The 11-term low-pass filtering (Trenberth, 1984) has been employed to remove high-frequency variability. The band-pass filter used is that of Murakami (1979).

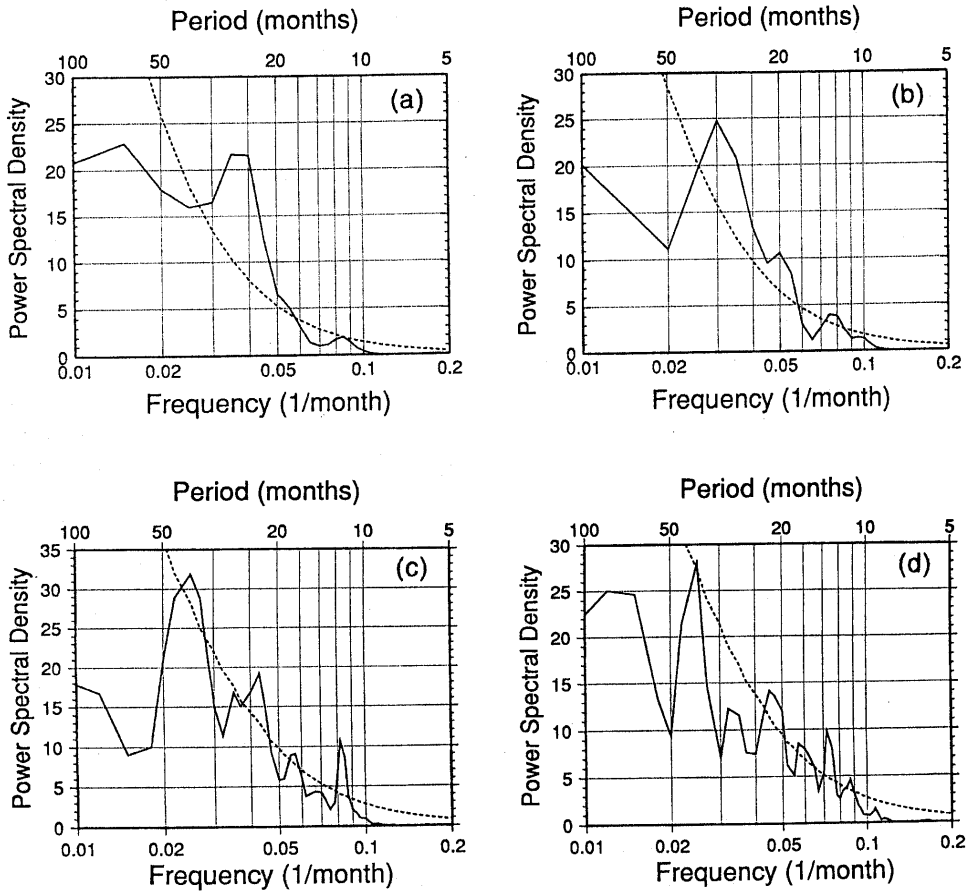


Fig. 3. Power spectral densities of SST in the South China Sea (a), All-India rainfall (b), meridional wind component over the South China Sea (100–130°E, EQ-30°N) (c), and SLP difference between 80–110°E, 40–60°N and 160°E–170°W, 40–60°N (d). The time series of solid lines in Fig. 2 are employed for (a) and (b). The procedures of low-pass filtering for (c) and (d) are the same as in Fig. 2. The unit is month due to the use of normalized data, and the frequency interval is 0.005 month$^{-1}$, making use of the Hanning spectral window. The dotted lines indicate the 95 % significance level, based on the red noise spectra, which are calculated from the autocorrelation coefficient at lag 1.

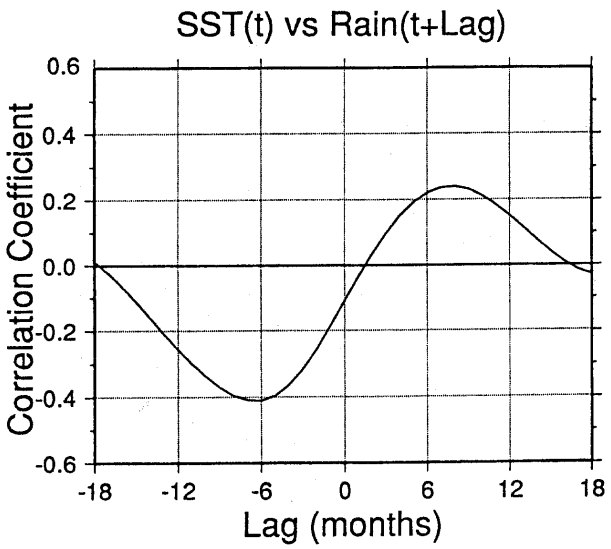


Fig. 4. Lag-correlations between the interannual variabilities of SST in the South China Sea and All-India rainfall. Negative lags indicate the All-India rainfall preceding the SST.

and 160°E–170°W, 40°N–60°N which correspond to the centers of Siberia High and Aleutian Low, respectively. Figures 3c and 3d imply that the BO of SST around the South China Sea is associated with the influence from mid-latitudes.

Shen and Lau (1995) strongly suggested that the ENSO and Asian monsoon are linked to each other through the biennial or quasi-biennial variation, rather than the more dominant 4–5-year period variation in the ENSO cycle. The present study focuses on and reveals the biennial relationship, while the problems of the relationship at the 4–5-year period still remain.

Figure 4 indicates the lag-correlations between the two time series represented by the solid lines in Fig. 2. Two pronounced peaks appear at lags of approximately plus and minus 6 months. That is, a maximum (0.24) appears at +8-months lag, and a minimum (−0.41) appears at −6-months lag. The absolute value of the minimum is larger than the maximum. That is, the linear relationship between the All-India rainfall and the following half year SST in the South China Sea is stronger than the relationship to the preceding half year.

Each time series denoted by the solid lines in Fig. 2 was separated into yearly series and superimposed on a figure having a period of one calendar year to investigate the seasonality of the interannual variabilities (Fig. 5). The maximum amplitude tends to appear during the northern winter as seen in Fig. 5a, while that for the All-India rainfall tends to appear in the summer (Fig. 5b). The two interannual variabilities in which the 2–3-year period component is dominant appear to have strong seasonal phase locking. The seasonality depicted in Fig. 5a strongly suggests that the interannual variability of SST around the South China Sea is controlled by the northeast winter monsoon (NEWM). The powers detected in Figs. 3c and 3d also support the suggestion.

The results shown here lead to the following BO relationship between the interannual variabilities of the SST around the South China Sea and the Indian southwest monsoon (ISWM) detected from the All-India rainfall. If positive SST anomalies appear around the South China Sea during the northern winter, the ISWM tends to become stronger than normal in the following summer. If the ISWM is stronger than normal during the northern summer, negative SST anomalies tend to appear around the South China Sea over the following winter. After this winter, the same progress continues, except with reversed signs, and the BO cycle is completed.

In order to estimate the persistence of the SST around the South China Sea during the northern winter, correlation coefficients are calculated between the northern winter SST and those in the following spring (0.75) and summer (0.59). Each correlation coefficient is statistically significant at the 99 % level (0.39). The correlation coefficient between the northern winter SST and those of the following autumn, however, is 0.24, which is not significant at the 99 % level. These correlation coefficients indicate that the South China Sea SST anomaly during the northern winter tends to persist to the following summer.

The positive lag-correlation between the ISWM and SST around the South China Sea (Fig. 4) may be explained by this persistent SST and the seasonal migration of convective activity around the maritime continent, as was shown by Meehl (1987, 1993). This process will be further discussed in Section 4.5. The mechanism for the negative lag-correlation, which may correspond to the negative correlation in Brier's conceptual BO model (Brier, 1978) is probably the key to the BO phase change in the ENSO/monsoon system.

## 4. Spatial and temporal structure of the biennial oscillation

A composite analysis is employed in this Section to reveal the typical spatial and temporal BO structure associated with the SST around the South China Sea. The composited years, *i.e.*, 1964, '66, '69, '71, '73, '75, '83, '85, and '88 (9 years), are chosen from years after 1960 with reference to the $+0.5\ \sigma$ in the band-pass filtered anomalies (dashed line) of the curve (a) in Fig. 2. For the maximum not less than $+0.5\ \sigma$ in the northern winter which spreads over 2 years, the composited years are represented by the latter year. The 30-year average,

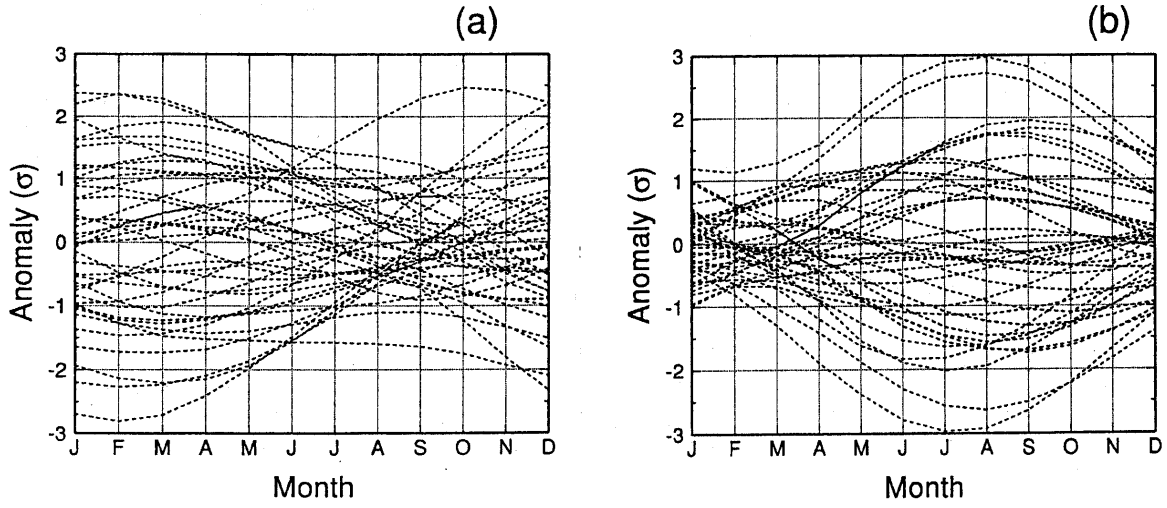


Fig. 5. The superposition of the annual time series of interannual variabilities of SST in the South China Sea (a) and All-India rainfall (b) over one calendar year. The time series used are the solid lines shown in Fig. 2, *i.e.*, for each year of 1948–91.

from 1961–1990 is employed as the climatology for the composited anomalies for each season. The results of the composite analysis of Meehl (1987) are similar to those presently obtained, although Meehl focused on the strong or weak Indian summer monsoon and employed different sample years. Each of the figures is shown in terms of a seasonal mean field due to the strong seasonal phase locking (Fig. 5).

*4.1 SST in the tropical central eastern Pacific*

Figures 6 show the seasonal change of composited SST anomalies in the Pacific and Indian Ocean basins from the northern spring (Fig. 6a) to the summer of the following year (Fig. 6f).

The most notable characteristic is the change of SST anomalies in the tropical central-eastern Pacific which corresponds to the relatively large area shown in Fig. 1. The northern spring is generally characterized by a neutral anomaly field (Fig. 6a), although a small area of positive anomaly appears in the equatorial eastern Pacific. The anomalous area develops into the tropical central Pacific during the northern spring (Fig. 6a) to autumn (Fig. 6c), and persists until the winter (Fig. 6d). In the following spring (Fig. 6e), the anomalous area rapidly reduces to the neutral state, and the sign of the anomaly changes from positive to negative by the time of next summer (Fig. 6f). The same patterns continue in the following seasons but with the sign reversed (not shown). It is difficult to perform statistical tests on the anomalies due to the small sample number, although each case, except for 1985, exhibits a similar anomalous development.

These features strongly suggest that the BO of the SST in the tropical central-eastern Pacific is closely related to the ENSO cycle. In fact, Tomita and Yasunari (1993) classified ENSO events into two types, *i.e.*, the biennial (BO) and longer period (about five years) types. The anomalous patterns shown here are basically comparable to the BO type of ENSO in the classification by Tomita and Yasunari (1993).

The Indian southwest monsoon (ISWM) tends to be weaker than normal during the preceding northern summer shown in Fig. 6b, and stronger than normal in the following summer (Fig. 6f) as discussed in the previous Section (Fig. 4). The development of the SST anomalies in the tropical central-eastern Pacific over the time period from northern spring (Fig. 6a) to autumn (Fig. 6b) can be attributed to the strength of ISWM through the Walker or east-west circulation (*e.g.*, Yasunari, 1990). Air-sea interaction in the tropical central-eastern Pacific also contributes to the development and persistence of the El Niño-or La Niña-like phenomena (*e.g.*, Philander, 1990). The mechanisms for the rapid decline and the reversing of the sign of the anomalies during the period from the northern winter (Fig. 6d) to summer (Fig. 6f) are probably the keys to the breakthrough of the "predictability barrier" in the ENSO cycle, which has been discussed by Webster and Yang (1992).

*4.2 SST around the South China Sea*

It should be further noted in Fig. 6 that a remarkable change in the SST anomalies occurred in the area around the South China Sea, including the region from the East China Sea to the Arafura and Timor Seas.

Before discussing the BO anomaly fields of SST, the normal seasonal changes around these regions should be recalled. From October to November, the SST in the South China Sea decreases to below 28°C due to the invasion of the northeast winter monsoon (NEWM). The SST is maintained at less than 28°C

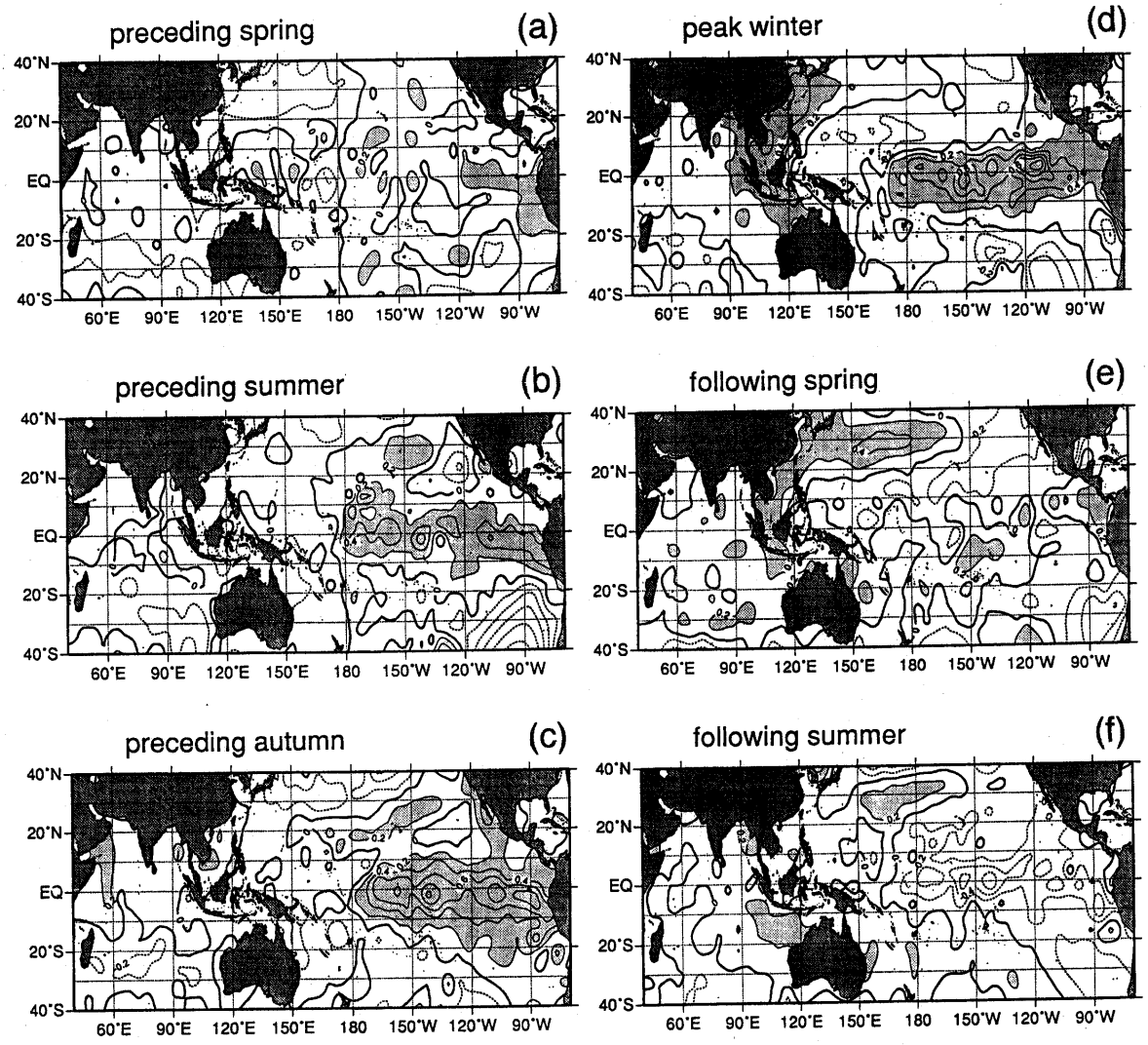


Fig. 6. Seasonal panels of composited SST anomalies. Composited years are 1964, '66, '69, '71, '73, '75, '83, '85, and '88 (9 years). For each season, the climatology used in the calculation of the anomalies is made from the 30-year average 1961-1990. The seasonal periods are sequentially shown from northern spring (a) to the summer of the next year (f). The contour interval is 0.2°C and areas greater than 0.2°C are shaded. The negative values are depicted by dashed contour lines.

until March when the NEWM begins to weaken. The SST exceeds 28°C over most of the region in April. During May, the NEWM is replaced by the southwest summer monsoon, coinciding with the onset of the summer monsoon. The SST further rises to a values of more than 29°C, persisting at around 28–29°C until October, and then begins to decrease by November (Sadler *et al.*, 1987a).

The seasonal variation of SST from the equator to north of Australia can be described as follows. The northwesterly wind that prevails until March is replaced by the southeasterly trade wind in April, though the high SST conditions of more than 28°C still prevail. The SST falls below 28°C, related to the enhancement of the southeasterly trade winds by June, with this low SST condition lasting until October. With the withdrawal of the southeasterly trade wind, the SST in the region rises to more than 28°C before November. By December, the southeasterly trade wind is replaced by the northwesterly wind from the Northern Hemisphere. The high SST condition of over 28°C continues until May of the next year (Sadler *et al.*, 1987b).

The BO anomaly fields of SST around the South China Sea were examined with reference to the seasonal changes. Negative SST anomaly areas of less than −0.2°C extend to the region off Japan and in the South China Sea (Fig. 6a). These areas disappear; that is, the neutral anomaly state appears in the following northern summer (Fig. 6b). This appearance is one season later than that in the tropical Pacific. During the northern autumn (Fig. 6c), positive SST anomalies appear in the South China Sea and further develop during the following winter

(Fig. 6d). This development can be attributed to the strength of the NEWM. This anomaly pattern persists to the following spring (Fig. 6e) and disappears by the next summer (Fig. 6f). The anomaly patterns are basically the same in both northern springs (Figs. 6a and 6e) and summers (Figs. 6b and 6f), except that the anomalies are of opposite sign.

*4.3 Wind anomalies from northern summer to spring*

The same composite analysis was performed on the wind anomalies to investigate the causes of the SST BO anomalies which appear around the South China Sea during the period from northern autumn to spring.

Figure 7a shows the wind anomalies during northern summer when positive SST anomalies develop in the tropical central-eastern Pacific (Fig. 6b). Westerly anomalies appear over the equatorial central-western Pacific with convergence also occurring in the equatorial region, especially from 160°W to 120°W. This anomaly pattern is favorable for the release of warm water which had accumulated in the western tropical Pacific, *i.e.*, the El Nino onset. The westerly anomalies persist to the following northern autumn (Fig. 7b), while meridional convergence further develops due to the appearance of southerly anomalies around 160°W, 15°S. Also noteworthy in Fig. 7b is the appearance of southerly anomalies from the East China Sea to the northern part of the South China Sea. It is plausible that this anomalous wind pattern causes the positive SST anomalies around the South China Sea, since it corresponds to the weak NEWM which suppresses evaporation from the ocean, the instability in the lower troposphere, and the mixing in the surface mixed layer of the ocean.

The most notable and interesting wind anomalies appear during the peak northern winter (Fig. 7c). Over most of the central North Pacific, easterly anomalies prevail. Especially strong northeasterly anomalies appear around 160°W, 20°N as a subset of the large anticyclonic circulation pattern over the mid-Pacific. Northerly anomalies, which may encourage convergence over the equatorial central Pacific, are dominant in the eastern and southeastern peripheries of the circulation. Westerly anomalies, which are probably the cause of the duration of the positive SST anomalies in the tropical central-eastern Pacific (Fig. 6d) remain to the immediate south of the equator in the central Pacific.

It is very important for the positive SST anomalies found around the South China Sea (Fig. 6d) that southerly anomalies (the weak NEWM) develop during the northern autumn to winter, from south of Japan to the South China Sea. Northeasterly anomalies in the tropical western Pacific and southeasterly anomalies on the northwest of Australia may also contribute to the positive SST anomalies around the maritime continent (Fig. 6d). The pattern of wind anomalies over the western Pacific prefers to strengthen the warm current under the region. There are no remarkable wind anomalies over the Indian Ocean and the eastern Pacific.

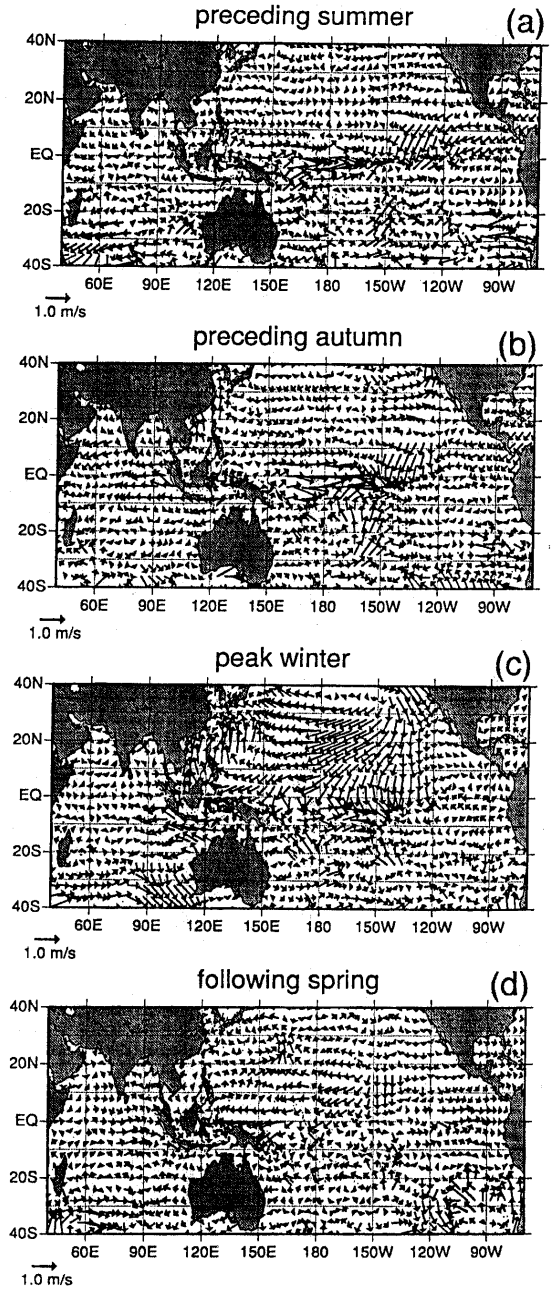


Fig. 7. Seasonal panels of composited wind anomalies. The composited years and the climatology for the anomalies are same as in Fig. 6. The seasonal periods are sequentially shown from northern summer (a) to the spring of the next year (d). The scale of wind anomaly vector is indicated at the bottom-left corner of each panel.

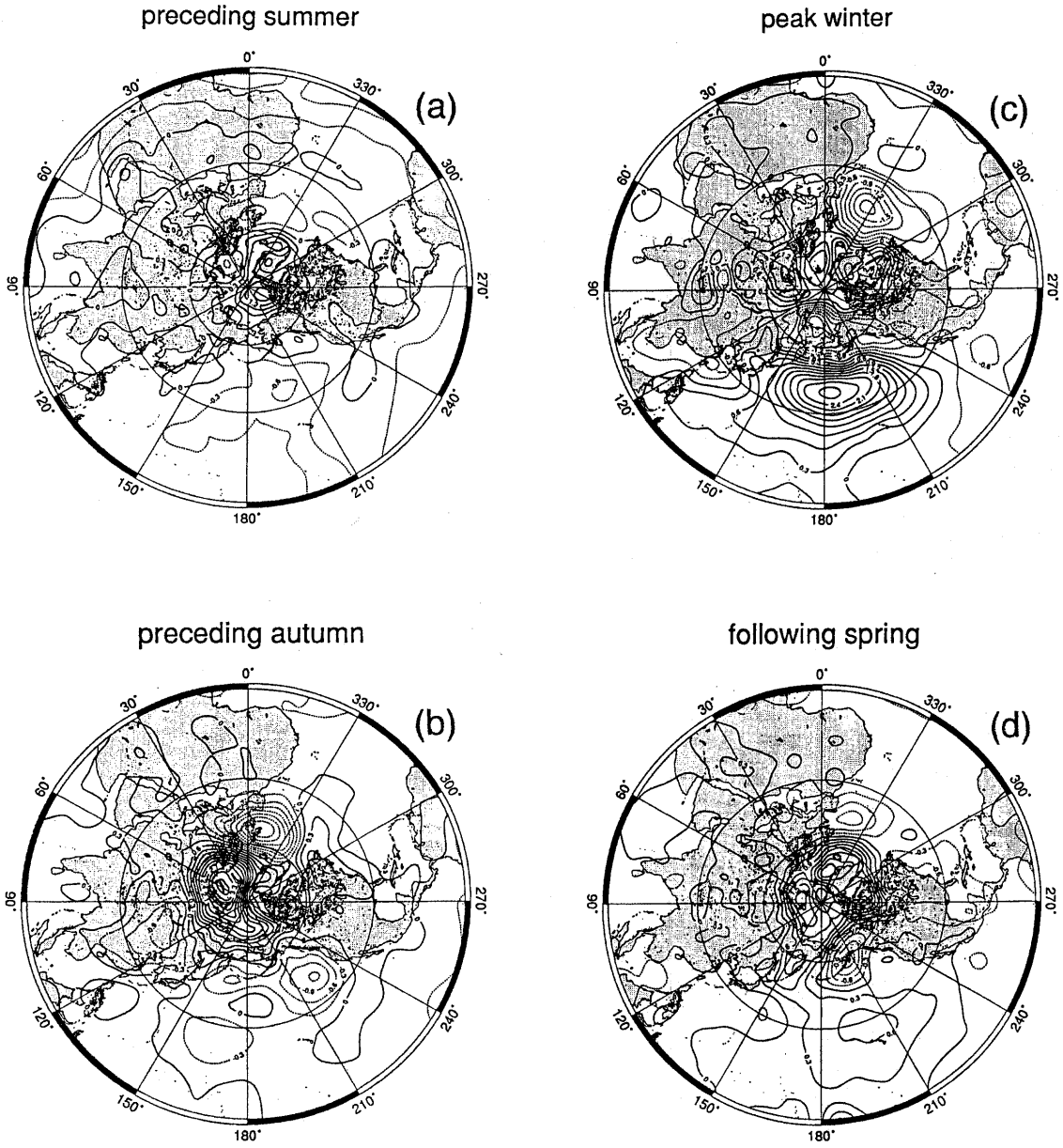


Fig. 8. Seasonal panels of composited SLP anomalies. The composited years and climatology for the anomalies are the same as in Fig. 6. The seasonal periods are sequentially shown from northern summer (a) to the spring of the next year (d). The contour interval is 0.3 hPa and the negative values are depicted by dashed contour lines.

The strong wind anomalies which appeared in Fig. 7c dissipate by the following northern spring (Fig. 7d), except for the northerly anomalies around 150°W, 10°N. There are, however, small easterly and westerly anomalies over the tropical western Pacific and tropical Indian Ocean, respectively. This anomaly pattern indicates stronger convergence and further implies stronger convective activity around the maritime continent.

*4.4 SLP anomalies from northern summer to spring*

In order to investigate the circulation patterns associated with the surface wind anomalies shown in Fig. 7, a composite analysis of SLP anomalies was applied to the Northern Hemisphere.

There are no remarkable anomaly patterns during the preceding northern summer (Fig. 8a), while small positive anomalies widely cover the Eurasian Continent. This may be related to a weaker than normal Asian summer monsoon, including the ISWM.

A notable SLP anomaly pattern appears in the region from the northeastern Atlantic to the eastern Eurasian Continent by the following autumn (Fig. 8b). This anomaly pattern is very similar to the Eurasian (EU) pattern, which is usually detected

in the 500 hPa height anomalies of the northern winter (Barnston and Livezey (1987)), and controls the snowfall on the Eurasian Continent (Morinaga, 1992). The negative SLP anomalies over the eastern Eurasian Continent are favorable for southerly wind anomalies (Fig. 7b) and, therefore, the positive SST anomalies around the South China Sea (Fig. 6c).

During the peak winter (Fig. 8c), the positive SLP anomaly centered over the North Pacific, corresponds to the anticyclonic circulation pattern that appeared in the wind anomaly field (Fig. 7c). This anomaly center is probably excited by positive SST anomalies in the tropical central-eastern Pacific (Fig. 6d) through the remote Rossby wave response, as in the Pacific-North American (PNA) pattern (*e.g.*, Horel and Wallace, 1981). The wave train, however, stretches from the North Pacific to the North Atlantic. The SLP anomaly pattern may correspond to the BO of the action centers detected by Angell *et al.* (1969). The anomaly centered over the North Pacific contributes to the northward shift and weakening of the Aleutian Low which in turn contributes to the weakening of the NEWM. With the southward extension of negative anomalies to the eastern Eurasian Continent, the southwest part of this SLP center acts to maintain the prevailing northerly wind of the NEWM. The EU like anomaly pattern which appeared in the preceding autumn (Fig. 8b) disappears, except for the negative anomalies over the eastern Eurasian Continent.

No remarkable SLP anomaly patterns occur in the following northern spring (Fig. 8d). A large positive anomaly center which appeared over the North Pacific during the preceding winter (Fig. 8c) appears to be weakened and shift southeastward. The anomaly pattern of the eastern Eurasian Continent completely disappears by this season. The negative anomalies appearing over the South China Sea may correspond to stronger than normal convection there.

The negative SLP anomalies over the eastern Eurasian Continent persist during the northern autumn to winter, while positive anomalies over the North Pacific persist during the northern winter to spring. The large southerly wind anomalies tend to appear during northern winter because the appearances of the anomalies overlap in this season.

### *4.5 OLR anomalies from northern autumn to summer*

The same composite analysis was then applied to the OLR data in order to discuss the BO phase change of the anomalous convective activity around the maritime continent during the period from the northern autumn to the following summer. The OLR is a good measure of convective activity in the tropics, where the smaller values correspond to lower temperatures, namely, the higher or stronger convection. The composite years were chosen after 1973, *i.e.*, 1975, '83, '85, '88 (4 years). The sample number is smaller than that of the previous composite analyses due to the shorter period of available data (14 years). The climatology for the anomalies was determined by a 14-year average, from 1975 to 1989 (except 1978) for each season.

During the northern autumn (Fig. 9a), positive OLR anomalies appear over the maritime continent, while negative anomalies are found in the tropical central-eastern Pacific. The band of negative anomalies from the central to eastern Pacific, near 5°N, corresponds to the stronger convection occurring in the intertropical convergence zone (ITCZ) and its southward shift. The anomalous stronger convection over the tropical central-eastern Pacific is probably due to the air-sea interaction with the positive SST anomalies associated with this region (Fig. 6c). Negative OLR anomalies also appear over the tropical Indian Ocean. These results strongly suggest that the Walker circulation is weaker than normal.

The positive OLR anomalies have strengthened over the maritime continent by the northern winter (Fig. 9b), while negative anomalies exist over the entire equatorial Pacific area. The negative OLR anomalies are attributed to the remaining positive SST anomalies in the tropical central-eastern Pacific (Fig. 6d). A Walker circulation weaker than that which occurred in the preceding autumn can be expected.

The reasons for the non-appearance of negative OLR anomalies, namely the stronger convective regions, over the positive SST anomalies around the maritime continent may be given as follows. A weaker NEWM is favorable for suppressing both the evaporation from the sea surface and the instability in the lower troposphere around the maritime continent. The anomalous descending flow of a weaker Walker circulation still prevails, which also suppresses convection. This weaker convective activity around the maritime continent may further contribute to the positive SST anomalies through radiative heating.

Notable changes occur in the following northern spring (Fig. 9c), after the season of the NEWM. Positive OLR anomalies are replaced by negative anomalies over the maritime continent, while the positive anomalies appear to shift to the tropical central Pacific. The drastic changes during the northern spring may also correspond to the seasonal migration of the convection center around the maritime continent, which has been previously discussed by Meehl (1987, 1993). The positive OLR anomaly band near 5°N in the Pacific indicates a weaker than normal ITCZ, though the large but weak negative anomaly area has yet to appear in the tropical southern Pacific. The negative anomalies off eastern

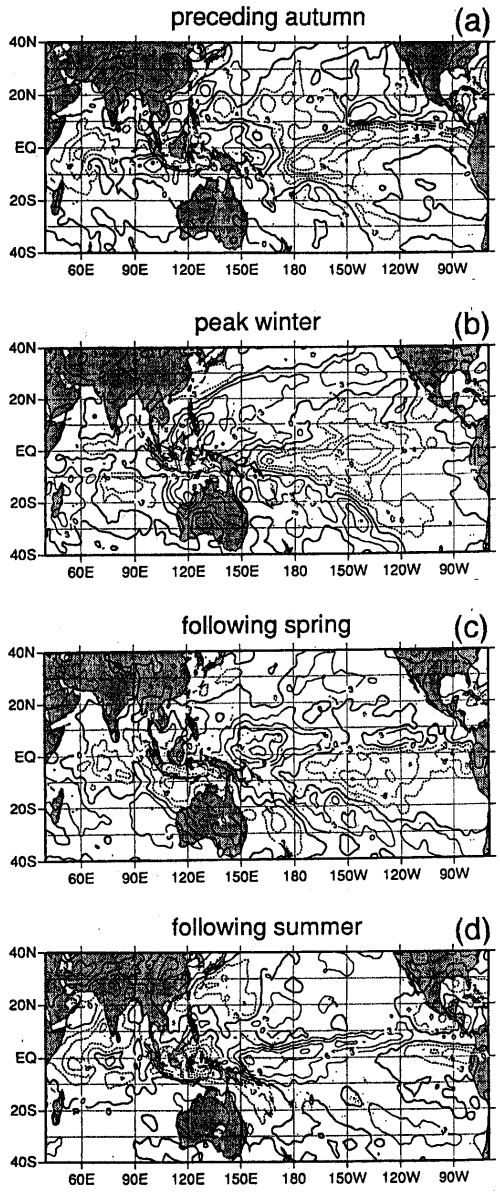


Fig. 9. Seasonal panels of composited OLR anomalies. Composited years are 1975, '83, '85, and '88 (4 years). The climatology for the anomalies was taken from a 14-year average, 1975 to 1989 (except 1978) for each season. The seasonal periods are sequentially shown from northern autumn (a) to the summer of the next year (d). The contour interval is 3 W/m$^2$ and the negative values are depicted by dashed contour lines.

Australia indicate a stronger South Pacific convergence zone (SPCZ). It is important for the BO phase change that the NEWM has a negative correlation to the SST around the South China Sea, and positive correlation to the convective activity around the maritime continent. These correlations are likely to set the conditions for the drastic convection change around the maritime continent during the northern spring.

The negative anomalies which had extended over the maritime continent and tropical Indian Ocean during the following northern spring (Fig. 9c) appear to be strengthened and shift northward by summer (Fig. 9d). These anomalies are probably related to a stronger ISWM. Positive anomalies prevail in the central tropical Pacific and the band area of the ITCZ. The Walker circulation seems to be stronger than normal, and a stronger SPCZ appears in this season.

## 5. Conclusions

The present study has revealed that the northeast winter monsoon (NEWM) plays an important role in the BO of the ENSO/monsoon system. Over the period of time from the northern autumn to winter, remarkable wind anomalies which indicate the anomalous weakening of the NEWM, appear over the area south of Japan to the South China Sea. This anomalous state is also confirmed by the SLP anomaly gradient between the negative anomalies over the southeastern Eurasian Continent and the positive anomalies in the western tropical Pacific. The former appears to have its origin in the EU pattern of the northern autumn, while the latter seems to be a part of the large positive anomaly centered over the north Pacific during the winter. This anomalous center, which is probably part of the modulated PNA pattern, also exerts influence on the strength and meridional shift of the Aleutian Low. The SST anomalies around the South China Sea change sign during the northern autumn, reaching a maximum in the winter and remain the anomaly until the summer, which closely reflect the strength of the NEWM. The convective activity over the maritime continent exhibits a distinct seasonal excursion, northwestward during the period from the northern winter to summer, and southeastward from summer to winter. The prolonged SST anomalies around the South China Sea tend to induce the phase change of the BO in the ENSO/monsoon system during the northern spring to summer, by controlling the strength of the convective activity in the region.

Based on the observed information in the present study, a possible sequence for the seasonal processes of the BO of the ENSO/monsoon system is proposed as follows (Fig. 10). When the Indian southwest monsoon (ISWM) is weaker than normal during the northern summer, the Walker circulation is also weaker than normal, with inactive convection around the maritime continent. The El Niño-like phenomenon of the BO is likely to be excited by the westerly wind anomalies over the tropical central-western Pacific which are associated with this weaker Walker circulation (*cf.* Yasunari, 1990),

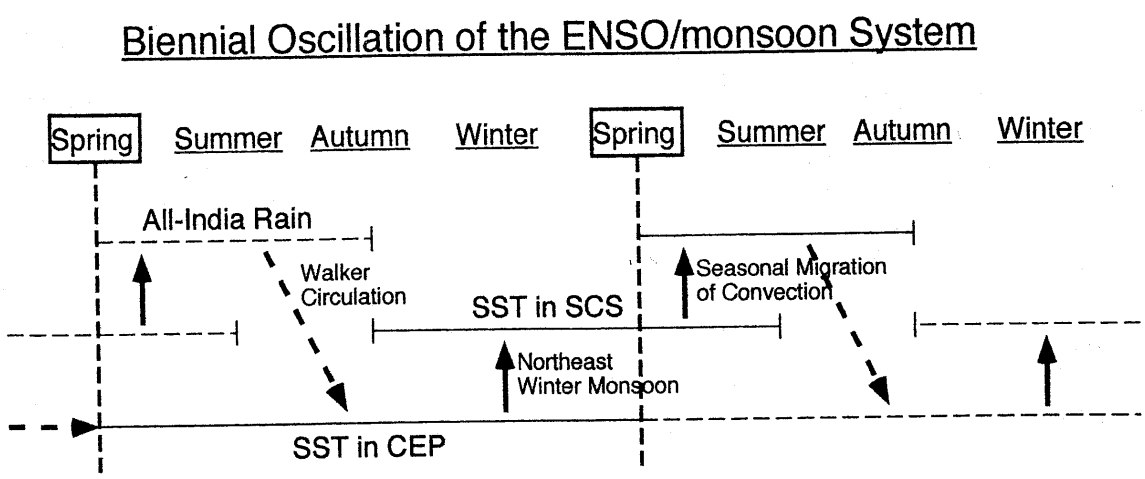


Fig. 10. A schematic diagram illustrating the biennial cycle of the ENSO/monsoon system. The thin solid and dashed lines indicate the periods of positive and negative anomaly, while the thick solid and dashed vectors indicate the positive and negative correlations, respectively. Abbreviations SCS and CEP denote the South China Sea and the central equatorial Pacific.

and develops through the air-sea interaction (*cf.* Philander, 1990). The positive SST anomalies of the El Niño phase develop in the central and eastern tropical Pacific during the period from the northern summer to winter.

The Rossby wave, excited by the SST anomalies, forms the PNA pattern in the northern winter (*cf.* Horel and Wallace, 1981). The modulated SLP anomalies of this PNA pattern form the large positive anomaly centered over the central North Pacific. The atmospheric circulation associated with this anomaly center appears to be coupled with the weakening of the NEWM. The weaker NEWM causes the positive SST anomalies around the South China Sea.

After the NEWM ends, the seasonal migration of convective activity around the maritime continent is strengthened by the positive SST anomalies around the South China Sea. Stronger convection may contribute to stronger ISWM activity. The La Niña-like phenomenon of the BO occurs due to the intensification of the Walker circulation. The La Niña phase persists to the next northern spring, with a similar seasonal processes but with the reversed signs of the anomaly patterns. Eventually, the cycle of the BO of the ENSO/monsoon system is completed.

In this cycle, the tropical-extratropical interaction through the northeast winter monsoon is the key to the phase change of the BO of the ENSO/monsoon system. The BO cycle may be supplemented by the wind curl mechanism discussed by Masumoto and Yamagata (1991). This mechanism is prominent during the northern winter over the western tropical Pacific. In particular, east of the Philippines, closely responding to the NEWM (see Fig. 7c). This anomalous wind curl has the capability of regulating the decay of the El Niño events through Ekman pumping in the mixed layer of the ocean. Moreover, Lukas (1988) pointed out a BO signal in a western Pacific ocean current, *i.e.*, the Mindanao Current off the Philippines.

In any case, the BO mechanism proposed in this study is different from that of Meehl (1987, 1993, 1994) in the sense that the former mechanism has included the tropical-extratropical interaction due to the NEWM. Furthermore, the proposed mechanism also emphasizes the tropical air-sea interaction over and around the maritime continent. The present study completes the BO cycle by revealing the tropical-extratropical interaction of the region from Asia to the Pacific.

The SLP anomalies suggest that the heating or cooling over the Eurasian Continent, from the northern autumn to winter, also plays an important role in the phase change of the BO of the ENSO/monsoon system, which has been discussed by Yasunari and Seki (1992) and Meehl (1994) (see Fig. 8b). Numerous previous studies have confirmed the significant negative correlation between the Eurasian snow cover and the following ISWM activity (Hahn and Shukla, 1976; Dey and Bhanu Kumer, 1982; Dickson, 1984). Li (1994) has also confirmed the BO of the snow cover as being dominant, and discussed the phase relation between the snow cover and the BO phase of the ISWM activity.

The effective anomaly pattern of SLP over the eastern part of the Eurasian Continent in northern autumn and winter may be induced by the cooling or heating associated with the anomalons snow cover. Evidence has also been provided that the intensification of the NEWM, perhaps due to the Eurasian snow cover during northern autumn and winter, contributes to the BO of the ENSO/monsoon system. The NEWM is closely related to the PNA and west-

ern Pacific (WP) patterns of the Northern Hemisphere 500 hPa height anomalies (*cf.* Kawamura, 1988). The Eurasian snow cover is strongly controlled by the atmospheric Eurasian (EU) pattern (Morinaga, 1992). Further studies are necessary to clarify the BO mechanism in the extratropics, its interaction with that in the tropics, and to thoroughly understand the complex BO processes in the climate system.

## Acknowledgments

The authors are grateful to Prof. T. Murakami of the University of Hawaii, Dr. G. A. Meehl of the National Center for Atmospheric Research, and Prof. M. Yanai of the University of California, Los Angeles for their advice, comments, and useful suggestions. This study has been supported by a grant-in-aid from the Japan Society for the Promotion of Sciences, and supported in part by the National Oceanic and Atmospheric Administration under Grant NA56GP0203.

## References

Ananthakrishnan, R. and A. Thiruvengadathan, 1966: Biennial oscillation in the equatorial troposphere. *Nature*, **207**, 1443.

Angell, J.K., J. Korshover and T.H. Carpenter, 1966: Note concerning the period of the quasi-biennial oscillation. *Mon. Wea. Rev.*, **94**, 319–323.

Angell, J.K. and J. Korshover, 1968: Additional evidence for quasi-biennial variations in tropospheric parameters. *Mon. Wea. Rev.*, **96**, 778–784.

Angell, J.K., J. Korshover and G.F. Cotten, 1969: Quasi-biennial variations in the "centers of action." *Mon. Wea. Rev.*, **97**, 867–872.

Angell, J.K. and J. Korshover, 1977: Variation in size and location of the 300 mb north circumpolar vortex between 1963 and 1975. *Mon. Wea. Rev.*, **105**, 20–25.

Barnett, T.P., 1983: Interaction of the monsoon and Pacific trade wind system at interannual time scales. Part I: The equatorial zone. *Mon. Wea. Rev.*, **111**, 756–773.

Barnett, T.P., 1991: The interaction of multiple time scales in the tropical climate system. *J. Climate*, **4**, 269–285.

Barnston, A.G. and R.E. Livezey, 1987: Classification, seasonality and persistence of low frequency atmospheric circulation patterns. *Mon. Wea. Rev.*, **115**, 1083–1126.

Brier, C.W., 1978: The quasi-biennial oscillation and feedback processes in the atmosphere-ocean-earth system. *Mon. Wea. Rev.*, **106**, 938–946.

Dey, B. and O.S.R.U. Bhanu Kumar, 1982: An apparent relationship between Eurasian spring snow cover and the advance period of the Indian Summer Monsoon. *J. Appl. Meteor.*, **21**, 1929–1932.

Dickson, R.R., 1984: Eurasian snow cover versus Indian monsoon rainfall —An extension of the Hahn-Shukla results. *J. Clim. Appl. Meteor.*, **23**, 171–173.

Ebdon, R.A., 1975: The quasi-biennial oscillation and its association with tropospheric circulation patterns. *Meteor. Mag.*, **104**, 282–297.

Fein, J.S. and P.L. Stephens, 1987: *Monsoons.* A Wiley-Interscience publication, 3–32

Hahn, D.G. and J. Shukla, 1976: An apparent relationship between Eurasian snow cover and Indian Monsoon raifall. *J. Atmos. Sci.*, **33**, 246–262.

Hanawa, K., R. San-nomiya and Y. Tanimoto, 1995: Static relationship between anomalies of SSTs and air-sea heat fluxes in the North Pacific. *J. Meteor. Soc. Japan*, **73**, 757–763.

Horel, J.D. and J.M. Wallace, 1981: Planetary-scale atmospheric phenomena associated with the Southern Oscillation. *Mon. Wea. Rev.*, **109**, 813–829.

Iwasaka, N. and K. Hanawa, 1990: Climatologies of marine meteorological variables and surface fluxes in the North Pacific computed from COADS. *Tohoku. Geophys. Journal.*, **33**, 185–239.

Joseph, P.V., B. Liebmann and H.H. Hendon, 1991: Interannual variability of the Australian summer monsoon onset: Possible influence of Indian summer monsoon and El Nino. *J. Climate*, **4**, 529–538.

Joseph, P.V., J.K. Eischeid, and R.J. Pyle, 1994: Interannual variability of the onset of the Indian summer monsoon and its association with atmospheric features, El Nino, and sea surface temperature anomalies. *J. Climate*, **7**, 81–105.

Kawamura, R., 1988: The interaction between winter monsoon activities in East Asia and sea surface temperature variations over the western Pacific Ocean. *Geograph. Rev. Japan*, **61** (Ser. A), 469–484 (in Japanese with English abstract and captions).

Lau, K.M. and P.J. Sheu, 1988: Annual cycle, quasi-biennial oscillation, and Southern Oscillation in global precipitation. *J. Geophys. Res.*, **93**, 10975–10988.

Li, C., 1994: Interannual variability of the Asian summer monsoon and its relationships with ENSO and Eurasian snow cover. Ph.D. dissertation, Univ. of California, 197p.

Lukas, R., 1988: Interannual fluctuations of the Mindanao Current inferred from sea level. *J. Geophys. Res.*, **93**, 6744–6748.

Masumoto, Y. and T. Yamagata, 1991: The response of the western tropical Pacific to the Asian winter monsoon: The generation of the Mindanao Dome. *J. Phys. Oceanogr.*, **21**, 1386–1398.

Meehl, G.A., 1987: The annual cycle and interannual variability in the tropical Pacific and Indian Ocean regions. *Mon. Wea. Rev.*, **115**, 27–50.

Meehl, G.A., 1993: A coupled air-sea biennial mechanism in the tropical Indian and Pacific regions: Role of the ocean. *J. Climate*, **6**, 31–41.

Meehl, G.A., 1994: Coupled land-ocean-atmosphere processes and South Asian monsoon variability. *Science*, **266**, 263–267.

Mooley, D.A. and B. Parthasarathy, 1984: Fluctuations in All-India summer monsoon rainfall during 1871–1978. *Climatic Change*, **6**, 287–301.

Mooley, D.A. and J. Shukla, 1987: Variability and forecasting of the summer monsoon rainfall over India.

*Monsoon Meteorology*, C.P. Chang and T.N. Krishnamurti, Eds., Oxford Univ. Press, 26–59.

Morinaga, Y., 1992: Interactions between Eurasian snow cover and the atmospheric circulations in the northern hemisphere. Ph.D. dissertation, Institute of geoscience, Univ. of Tsukuba, 78p.

Murakami, M., 1979: Large-scale aspects of deep convective activity over the GATE area. *Mon. Wea. Rev.*, **107**, 994–1013.

Newell, R.E., J.W. Kidson, and D.G. Vincent, 1969: Annual and biennial modulations in the tropical Hadley cell circulation. *Nature*, **222**, 76–78.

Nicholls, N., 1978: Air-sea interaction and the quasi-biennial oscillation. *Mon. Wea. Rev.*, **106**, 1505–1508.

Parthasarathy, B., K. Rupa Kumar and A.A. Munot, 1991: Evidence of secular variations in Indian monsoon rainfall-circulation relationships. *J. Climate*, **4**, 927–938.

Parthasarathy, B., A.A. Munot and D.R. Kothawale, 1994: All-India monthly and seasonal rainfall series: 1871–1993. *Theor. Appl. Climatol.*, **49**, 217–224.

Philander, S.G., 1990: *El Nino, La Nina, and the Southern Oscillation.* Academic press, 210–254.

Rasmusson, E.M. and T.H. Carpenter, 1982: Variations in tropical sea surface temperature and surface wind fields associated with the Southern Oscillation/El Nino. *Mon. Wea. Rev.*, **110**, 354–384

Rasmusson, E.M. and T.H. Carpenter, 1983: The relationship between eastern equatorial Pacific sea surface temperature and rainfall over India and Sri Lanka. *Mon. Wea. Rev.*, **111**, 517–528.

Rasmusson, E.M., X. Wang and C.F. Ropelewski, 1990: The biennial component of ENSO variability. *J. Mar. Sci.*, **1**, 71–96.

Ropelewski, C.F., M.S. Halpert and X. Wang, 1992: Observed tropospheric biennial variability and its relationship to the Southern Oscillation. *J. Climate*, **5**, 594–614.

Sadler, J.C., M.A. Lander, A.M. Hori and L.K. Oda, 1987a: Tropical Marine Climatic Atlas. Volume I: Indian Ocean and Atlantic. Univ. of Hawaii, Dept. of Meteorology, UHMET, 87–01.

Sadler, J.C., M.A. Lander, A.M. Hori and L.K. Oda, 1987b: Tropical Marine Climatic Atlas. Volume II: Pacific Ocean. Univ. of Hawaii, Dept. of Meteorology, UHMET 87–02.

Shen, S. and K.-M. Lau, 1995: Biennial oscillation associated with the East Asian summer monsoon and tropical sea surface temperatures. *J. Meteor. Soc. Japan*, **73**, 105–124.

Tomita, T. and T. Yasunari, 1993: The two types of ENSO. *J. Meteor. Soc. Japan*, **71**, 273–284.

Trenberth, K., 1980: Atmospheric quasi-biennial oscillations. *Mon. Wea. Rev.*, **108**, 1370–1377.

Trenberth, K., 1984: Signal versus noise in the Southern Oscillation. *Mon. Wea. Rev.*, **112**, 326–332.

Trenberth, K. and D.J. Shea, 1987: On the evolution of the Southern Oscillation. *Mon. Wea. Rev.*, **115**, 3078–3096.

Webster, P.J. and S. Yang, 1992: Monsoon and ENSO: Selectively interactive systems. *Quart. J. Roy. Meteor. Soc.*, **118**, 877–926.

Xu, J.-S., 1992: On the relationship between the stratospheric quasi-biennial oscillation and the tropospheric southern oscillation. *J. Atmos. Sci.*, **49**, 725–734.

Yasunari, T., 1987: Global structure of the El Nino/Southern Oscillation. Part II. Time evolution. *J. Meteor. Soc. Japan*, **65**, 81–102.

Yasunari, T., 1989: A possible link of the QBOs between the stratosphere, troposphere and sea surface temperature in the tropics. *J. Meteor. Soc. Japan*, **67**, 483–493.

Yasunari, T., 1990: Impact of Indian monsoon on the coupled atmosphere/ocean system in the tropical Pacific. *Meteor. & Atmos. Phys.*, **44**, 29–41.

Yasunari, T., 1991: "The monsoon year" - A new concept of the climatic year in the tropics-. *Bull. Amer. Meteor. Soc.*, **72**, 1331–1338.

Yasunari, T. and Y. Seki, 1992: Role of the Asian monsoon on the interannual variability of the global climate system. *J. Meteor. Soc. Japan*, **70**, 177–189.

# ENSO/モンスーンシステムの2年周期振動における冬季北東モンスーンの役割

冨田智彦
（UCLA大気科学科）
安成哲三
（筑波大学地球科学系）

ENSO/モンスーンシステムの2年周期変動の実態とそのメカニズムに関する考察を海面水温、海面風、海面補正気圧、そして外向き長波放射データを用いて診断的に行った。

海洋大陸域付近の世界で最も強い対流活動によって主に維持されているENSO/モンスーンシステムには、約2年周期(BO)の変動が卓越し、このBOは、北半球の春にその偏差状態を反転させる傾向がある。一方、南シナ海付近の海面水温の変動にもBOが顕著に見られ、この海面水温の偏差の反転は、ENSO/モンスーンシステムの変動に対し約半年先行している。秋から冬にかけての北東モンスーンの強弱により形成され、次の夏まで持続する。

海洋大陸上の対流活動のBOは、南シナ海付近の海面水温のBOと強く相互作用しているようである。すなわち、海洋大陸での対流活動の強弱は、Walker循環を介し北半球の夏から冬にかけて、中東部太平洋熱帯域の海面水温偏差を規制する。この海面水温偏差は、大気のテレコネクションによって中高緯度の循環場を規制し、冬季北東モンスーンの強弱をも規制する。さらにこの冬季北東モンスーンの強弱は、南シナ海付近の海面水温の偏差を通して、引き続く春から夏の対流活動の偏差を反転させ、このBOサイクルは閉じると考えられる。このように熱帯-中緯度相互作用がENSO/モンスーンシステムの2年周期変動にとって本質的に重要な役割を担っている可能性の高いことが示唆された。